

AD-A232 679

MASTER COPY

KEEP THIS COPY FOR REPRODUCTION PURPOSES

REPORT DOCUMENTATION PAGE

Form Approved
OMB No. 0704-0188

(2)

Public reporting burden for this collection of information is estimated to average 1 hour per response, including the time for reviewing instructions, searching existing data sources, gathering and maintaining the data needed, and completing and reviewing the collection of information. Send comments regarding this burden estimate or any other aspect of this collection of information, including suggestions for reducing the burden, to Washington Headquarters Services, Directorate for Information Operations and Reports, 1215 Jefferson Davis Highway, Suite 1204, Arlington, VA 22202-4302, and to the Office of Management and Budget, Paperwork Reduction Project (0704-0188), Washington, DC 20503.

1. AGENCY USE ONLY (Leave blank)	2. REPORT DATE	3. REPORT TYPE AND DATES COVERED	
	1-17-91	Reprint	
4. TITLE AND SUBTITLE		5. FUNDING NUMBERS	
Enhanced Spontaneous Emission from GaAs Quantum Wells in Monolithic Microcavities		DAAL03-89-C-0001	
6. AUTHOR(S)		8. PERFORMING ORGANIZATION REPORT NUMBER	
H. Yokoyama, K. Mishi, T. Anan, H. Yamada, S.D. Brorson, E.P. Ippen			
7. PERFORMING ORGANIZATION NAME(S) AND ADDRESS(ES)		9. SPONSORING/MONITORING AGENCY NAME(S) AND ADDRESS(ES)	
Research Laboratory of Electronics Massachusetts Institute of Technology 77 Massachusetts Avenue Cambridge, MA 02139		U. S. Army Research Office P. O. Box 12211 Research Triangle Park, NC 27709-2211	
		10. SPONSORING/MONITORING AGENCY REPORT NUMBER	
		ARU 26213.81-EL	
11. SUPPLEMENTARY NOTES <hr/> The views, opinions and/or findings contained in this report are those of the author(s) and should not be construed as an official Department of the Army position, policy, or decision, unless so designated by other documentation.			
12a. DISTRIBUTION/AVAILABILITY STATEMENT Approved for public release; distribution unlimited.		12b. DISTRIBUTION CODE G	
13. ABSTRACT (Maximum 200 words) <hr/> Enhanced spontaneous emission has been observed with wavelength-sized monolithic Fabry-Perot cavities containing GaAs quantum wells. With an on-resonance cavity structure, the photoluminescence intensity increases in the cavity axis direction, and the spontaneous emission lifetime is experimentally found to decrease.			
14. SUBJECT TERMS		15. NUMBER OF PAGES	
		16. PRICE CODE	
17. SECURITY CLASSIFICATION OF REPORT UNCLASSIFIED	18. SECURITY CLASSIFICATION OF THIS PAGE UNCLASSIFIED	19. SECURITY CLASSIFICATION OF ABSTRACT UNCLASSIFIED	20. LIMITATION OF ABSTRACT UL

NSN 7540-01-280-5500

91 2 19 003

Standard Form 298 (Rev. 2-89)
Prescribed by ANSI Std Z39-18
298-102

Enhanced spontaneous emission from GaAs quantum wells in monolithic microcavities

H. Yokoyama,^{a)} K. Nishi, T. Anan, and H. Yamada

Opto-Electronics Research Laboratories, NEC Corporation, 4-1-1, Miyazaki, Miyamae-ku, Kawasaki 213, Japan

S. D. Brorson and E. P. Ippen

Department of Electrical Engineering and Computer Science and Research Laboratory of Electronics, Massachusetts Institute of Technology, Cambridge, Massachusetts 02139

(Received 18 July 1990; accepted for publication 1 October 1990)

Enhanced spontaneous emission has been observed with wavelength-sized monolithic Fabry-Perot cavities containing GaAs quantum wells. With an on-resonance cavity structure, the photoluminescence intensity increases in the cavity axis direction, and the spontaneous emission lifetime is experimentally found to decrease.

Following the recent reports of altered spontaneous emission in optical cavities,¹ attention has turned to utilizing this effect in semiconductor optical devices. For example, the utilization of inhibited spontaneous emission has been proposed to create diode lasers having extremely low threshold current.² It has also been recently reported that the spontaneous emission rate of optically thin GaAs/AlGaAs double heterostructures depends on substrate materials.³ However, until now, there have been few studies of optical cavity effects on semiconductors, possibly because of the difficulty of fabricating the appropriate cavity structures with these materials. For broad emission bandwidth semiconductors, the spontaneous emission rate change can be observed only when the dimensions of the cavity are on the order of a wavelength, in contrast to atomic beam experiments.⁴ In this letter we report two experiments designed to detect enhanced spontaneous emission from a semiconductor multiple quantum well (MQW) sample embedded in a monolithic microcavity. In the first experiment, the enhancement is detected as an increase in the spectrally integrated photoluminescence (PL) intensity emitted from the sample perpendicular to the MQW layers. In the second experiment, we observe the change in the spontaneous emission lifetime of the MQW caused by the presence of the cavity.

The microcavity was fabricated by the epitaxial growth of both multi quantum well light-emitting active layers and multilayer reflectors on a GaAs substrate. This structure is basically a very short planar Fabry-Perot cavity structure, but with distributed feedback reflectors. The structure is schematically shown in Fig. 1. The active layer consists of a three-period multiple quantum well (MQW) structure having 6.5-nm-thick GaAs wells and Al_{0.3}Ga_{0.7}-As barriers of the same thickness, and enclosed by Al_{0.3}Ga_{0.7}-As spacer layers. The optical thickness of the active layer is $\lambda/2$. These MQW structures are not intentionally doped, and the background hole density is $\sim 10^{15} \text{ cm}^{-3}$. The use of a MQW structure is intended to shift the luminescence peak to shorter wavelengths ($\sim 830 \text{ nm}$), in order to exclude the

possibility of mistakenly detecting the GaAs substrate luminescence ($\sim 870 \text{ nm}$). One of a pair of reflectors is made from alternating quarter-wavelength layers of AlAs and Al_{0.3}Ga_{0.7}-As, with 20 pairs of these layers. Based on the layer matrix calculation method,⁵ it is estimated that this reflector yields a peak reflectivity $R_1 \sim 0.98$, flat over approximately 20 nm. Half of the sample wafer, hereafter called the "microcavity section" (MCS), is covered by a seven-layer ZnS/SiO₂ upper reflector having a reflectivity $R_2 \sim 0.9$ for the 740–900 nm wavelength region, while showing reflectivity of less than 0.1 for wavelengths shorter than 700 nm. It should be noted that although the whole active layer thickness is $\lambda/2$, the effective cavity length has been estimated to be approximately $\sim 3\lambda$ by a layer matrix simulation of the cavity resonance separation. This is mainly due to penetration of the cavity field into the epitaxial layer reflector. The other half of the wafer, hereafter called the "weak-cavity section" (WCS), has only one ZnS upper layer as an antireflection (AR) coating. Note that there is a weak cavity effect in this section because of the epitaxially grown reflector and the incomplete AR coating.

Calculating the change in spatially integrated spontaneous emission rate is quite difficult with such a distributed feedback structure. However, at least within a small solid angle around the cavity axis, a significant change in the

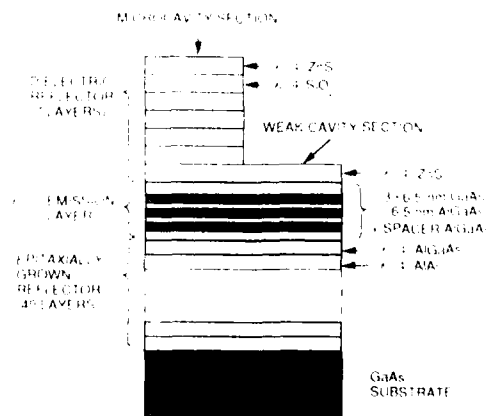


FIG. 1. Schematic of a microcavity MQW structure.

^{a)} On leave at the Research Laboratory of Electronics, Massachusetts Institute of Technology, Cambridge, MA 02139.

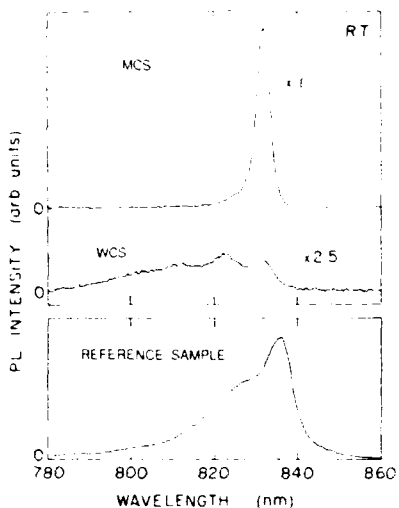


FIG. 2 PL spectra for a microcavity GaAs MQW structure. As a reference a PL spectrum for a MQW without reflectors is also shown. Excitation He-Ne laser light intensity is 1 kW cm^{-2} , with $\sim 24 \mu\text{m}$ focal spot diameter. PL detection solid angle is $\sim 10^{-2} \pi$.

emission intensity is expected.⁶ When a semiconductor is placed in a Fabry-Perot (FP) microcavity and only one FP mode exists within its emission width, the intensity ratio η for spectrally integrated emission into the cavity axis direction can be expressed as⁶

$$\eta = P(E'_0)\Delta E / P(E_0)\Delta P. \quad (1)$$

where $P(E)$ is the energy-dependent transition rate of the semiconductor at photon energy E , E'_0 and E_0 are respectively the photon energies at the cavity resonance peak and at the free-space emission peak, and ΔE and ΔP are respectively the FP mode separation, and the full width at half maximum (FWHM) of $P(E)$. Here we assume that the absorptive loss is negligible. If $E'_0 = E_0$, the emission intensity is enhanced by a ratio of $\sim \Delta E / \Delta P$. This shows that the spectrally integrated emission enhancement depends on the cavity mode separation (i.e., the optical thickness of a Fabry-Perot cavity). Note that if $E'_0 \neq E_0$ and $P(E_0)/P(E'_0) > \Delta E / \Delta P$, the microcavity causes the spontaneous emission into the cavity axis direction to be suppressed instead of enhanced. The electrodynamics of such Fabry-Perot cavities is discussed more fully in Ref. 7.

For both measurements, a small sample including both the MCS and WCS was extracted from a 40-mm-diam wafer. The static PL intensity measurements were carried out using He-Ne laser excitation ($\lambda = 633 \text{ nm}$). The focal spot diameter on the sample surface is estimated to be $\sim 24 \mu\text{m}$. To avoid cracking the coated dielectric layers, all the measurements were carried out at room temperature.

Figure 2 shows the static PL spectra for the sample. The reference spectrum was obtained from a MQW sample without any reflectors. Since this comes from another wafer, its amplitude should not be compared with those from the microcavity sample. (Its peak wavelength is also somewhat longer because the QW layers were slightly thicker.)

In the measurement, PL is detected along the axis perpendicular to the sample surface within a solid angle of $\sim 10^{-2} \pi$. The observed PL spectral width for the MCS is $\sim 4 \text{ nm}$ full width at half maximum (FWHM) around the lowest quantized electron-heavy hole transition. The PL spectrum for the WCS is modified by a residual cavity effect. The spectral shapes for both MCS and WCS do not change when the excitation intensity is varied from 1 kW cm^{-2} to $\sim 100 \text{ W cm}^{-2}$ (the detection limit for spectra). It should be noted that the MCS and WCS, from which PL data are obtained, are less than 1 mm distant from each other on the wafer in order to assure similarity of the layer thickness and the quality of the MQW.

Integration of the curves shown in Fig. 2 shows that the spectrally integrated PL intensity emitted into the cavity axis direction is increased by a factor of 3.6 by the microcavity. From (1) we estimate an expected enhancement factor of 7–8. Considering the absorption of the MQW, the observed enhancement factor of 3.6 seems to be reasonable.

It is important in these experiments to distinguish between stimulated and spontaneous emission. When the carrier density is less than 10^{18} cm^{-3} , net stimulated emission (stimulated emission rate > stimulated absorption rate) may not occur around the PL peak wavelengths.⁸ For our pumping intensity, we estimate the carrier density to be $\sim 10^{18} \text{ cm}^{-3}$. Thus, the light emission observed in the present experiment is due to spontaneous emission. Furthermore, even if the carrier density is increased to 10^{18} cm^{-3} , the gain induced in the MQW is optimistically 10^2 cm^{-1} , giving a single pass MQW gain of $\sim 4 \times 10^{-4}$ for the cavity axis direction. This value is much smaller than the mirror transmission loss $1 - \sqrt{R_1 R_2} \sim 0.06$. Finally, the single pass gain for the direction parallel to the MQW is ~ 0.3 with the present excitation diameter. Accordingly, the effect of stimulated emission is not important at this carrier density.

With samples extracted from other parts of the whole wafer, shifts of the microcavity resonance peak to long wavelengths have been observed. This peak is due to the slight change in the active layer thickness originating from the flux density gradient of the molecular beam during MBE growth. When the resonance peak occurs at a wavelength longer than 840 nm (off-resonance microcavity), the MCS emission intensity into the cavity axis becomes lower than that of the WCS section as expected, i.e., $P(E'_0)\Delta E / P(E_0)\Delta P < 1$ in (1).

Thus far, we have discussed changes of the PL intensity in the cavity axis direction. However, the presence of the cavity can also alter the total spontaneous emission rate (i.e., the actual radiative lifetime), analogously to the case of dye molecules encased in thin dielectric layers.^{1,9} We have demonstrated these effects with time-resolved PL measurements. In this experiment, an AlGaInP visible diode laser ($\lambda \approx 660 \text{ nm}$) excites the sample with a picosecond pulse of light; the decay of the emitted PL is monitored in time using the single photon counting technique.¹⁰ The measurements have also been carried out at room temperature. From the time-resolved PL measurement, the

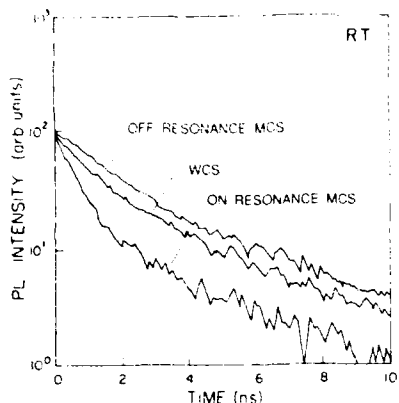


FIG. 3. Temporal variation of the spectrally integrated PL intensity for a GaAs microcavity. The decay times are estimated from the slope of the decay in the initial 2 ns portion of the curve.

nonradiative carrier lifetime of the MQW structure has been determined to be ~ 2 ns at room temperature. This indicates that the well/barrier interfacial recombination velocity is rather large. Although a radiative lifetime change cannot be observed at an initial carrier density lower than 10^{12} cm^{-3} because of the very short nonradiative lifetime, the lifetime difference between the MCS and WCS becomes comparable to the nonradiative case. As explained previously, the contribution of stimulated emission is quite unimportant even at this excitation condition in the present microcavity structure. In Fig. 3, the decay of the spectrally integrated PL intensity is shown for $\sim 10^{18} \text{ cm}^{-3}$ initial carrier density. The slope of the initial PL decay trace gives decay time constants of ~ 1 ns for the WCS and off-resonant MCS, and ~ 0.6 ns for the on-resonant MCS section. The observed initial decay time τ_I is related to the nonradiative decay time τ_{nr} , and the radiative decay time τ_{rad} by $1/\tau_I = 1/\tau_{nr} + 1/\tau_{rad}$. Although the estimated value of radiative lifetime τ_{rad} sensitively depends on the value of τ_{nr} , using the above relation and the measured nonradiative lifetime $\tau_{nr} \sim 2$ ns, we find radiative lifetimes around 2 ns for the WCS and the off-resonant MCS, and 1 ns for the on-resonant MCS, respectively. The 2 ns time is comparable to previously re-

ported values of radiative lifetimes in samples with carrier densities of 10^{18} cm^{-3} within a factor of 2.¹¹ The reduction of 1 ns directly reflects the spontaneous emission rate enhancement by the microcavity. Inhibition of the overall emission rate, if any is induced in this structure, is rather small in the present experiment. However, the experimental results demonstrate that an overall enhancement of the spontaneous emission rate is obtainable in the on-resonant MCS compared to the WCS.

In conclusion, our results show for the first time that spontaneous emission alteration is indeed obtainable when GaAs MQWs are incorporated in a planar microcavity. Specifically, the microcavity structure examined here caused both an increase of the spontaneous emission intensity in the cavity axis direction, as well as a change in the overall spontaneous emission lifetime. Although laser oscillation was not observed here because of the high loss cavity, similar alteration in spontaneous emission will certainly occur in the operation of recent surface emitting microcavity laser devices.

The authors are grateful to Professor H. A. Haus, Professor D. Kleppner, Dr. J. T. Hutton, and J. J. Childs (MIT), E. Yablonovitch (Bellcore), Dr. R. Lang (NEC), and Y. Yamamoto (NTT) for helpful discussions. Work at MIT was supported in part by Joint Services Electronics Program Contract DAAL03-89-C-0001.

- ¹F. De Martini, G. Innocenti, G. R. Jacobovitz, and P. Mataloni, Phys Rev Lett **59**, 2955 (1987); W. Jhe, A. Anderson, E. A. Hinds, D. Meschede, L. Moi, and S. Haroche, Phys. Rev. Lett. **58**, 666 (1987).
- ²E. Yablonovitch, Phys. Rev. Lett. **58**, 2059 (1987).
- ³E. Yablonovitch, T. J. Gmitter, and R. Bhat, Phys. Rev. Lett. **61**, 2546 (1988).
- ⁴D. J. Heinzen, J. J. Childs, J. E. Thomas, and M. S. Feld, Phys. Rev. Lett. **58**, 1320 (1987).
- ⁵H. Yokoyama, IEEE J. Quantum Electron. **QE-25**, 190 (1989).
- ⁶H. Yokoyama and S. D. Brorson, J. Appl. Phys. **66**, 4801 (1989).
- ⁷S. D. Brorson, H. Yokoyama, and E. P. Ippen, IEEE J. Quantum Electron. **26**, 1492 (1990).
- ⁸N. K. Dutta, J. Appl. Phys. **53**, 7211 (1982).
- ⁹K. H. Drexhage, in *Progress in Optics*, edited by E. Wolf (North-Holland, Amsterdam, 1974), Vol. XII, p. 165.
- ¹⁰H. Yokoyama, M. Fujii, M. Sugimoto, H. Iwata, K. Onabe, and T. Suzuki, *Springer Series in Chemical Physics Vol. 48: Ultrafast Phenomena*, edited by T. Yajima, K. Yoshihara, C. B. Harris, and S. Shioleya (Springer, Berlin, 1988).
- ¹¹T. Matsusue and H. Sakaki, Appl. Phys. Lett. **50**, 1429 (1987).

ACKNOWLEDGMENT	
(check one)	
NTIS REF ID: A	
1. AUTHOR'S NAME	
2. TITLE OF REPORT	
3. NAME OF CONTRACT OR GRANT NUMBER	
4. NAME OF FUNDING SOURCE	
5. NUMBER OF PAGES	
6. NUMBER OF FIGURES	
7. NUMBER OF TABLES	
8. NUMBER OF APPENDICES	
9. NUMBER OF REFERENCES	
10. NUMBER OF PICTURES	
11. NUMBER OF PLATES	
12. NUMBER OF DRAWINGS	
13. NUMBER OF SPECIMENS	
14. NUMBER OF VOLUMES	
15. NUMBER OF MICROFILMS	
16. NUMBER OF MICROCARDS	
17. NUMBER OF MICROFORMS	
18. NUMBER OF COMPUTER CARDS	
19. NUMBER OF COMPUTER DISKS	
20. NUMBER OF COMPUTER TAPE	
21. NUMBER OF OTHER	
22. NUMBER OF TOTAL	
23. NUMBER OF PAGES IN THIS FORM	
24. NUMBER OF PAGES IN THIS REPORT	
25. NUMBER OF PAGES IN THIS SECTION	
26. NUMBER OF PAGES IN THIS APPENDIX	
27. NUMBER OF PAGES IN THIS TABLE	
28. NUMBER OF PAGES IN THIS DRAWING	
29. NUMBER OF PAGES IN THIS PLATE	
30. NUMBER OF PAGES IN THIS MICROFORM	
31. NUMBER OF PAGES IN THIS COMPUTER CARD	
32. NUMBER OF PAGES IN THIS COMPUTER DISK	
33. NUMBER OF PAGES IN THIS COMPUTER TAPE	
34. NUMBER OF PAGES IN THIS OTHER	
35. NUMBER OF PAGES IN THIS SECTION	
36. NUMBER OF PAGES IN THIS APPENDIX	
37. NUMBER OF PAGES IN THIS TABLE	
38. NUMBER OF PAGES IN THIS DRAWING	
39. NUMBER OF PAGES IN THIS PLATE	
40. NUMBER OF PAGES IN THIS MICROFORM	
41. NUMBER OF PAGES IN THIS COMPUTER CARD	
42. NUMBER OF PAGES IN THIS COMPUTER DISK	
43. NUMBER OF PAGES IN THIS COMPUTER TAPE	
44. NUMBER OF PAGES IN THIS OTHER	
45. NUMBER OF PAGES IN THIS SECTION	
46. NUMBER OF PAGES IN THIS APPENDIX	
47. NUMBER OF PAGES IN THIS TABLE	
48. NUMBER OF PAGES IN THIS DRAWING	
49. NUMBER OF PAGES IN THIS PLATE	
50. NUMBER OF PAGES IN THIS MICROFORM	
51. NUMBER OF PAGES IN THIS COMPUTER CARD	
52. NUMBER OF PAGES IN THIS COMPUTER DISK	
53. NUMBER OF PAGES IN THIS COMPUTER TAPE	
54. NUMBER OF PAGES IN THIS OTHER	
55. NUMBER OF PAGES IN THIS SECTION	
56. NUMBER OF PAGES IN THIS APPENDIX	
57. NUMBER OF PAGES IN THIS TABLE	
58. NUMBER OF PAGES IN THIS DRAWING	
59. NUMBER OF PAGES IN THIS PLATE	
60. NUMBER OF PAGES IN THIS MICROFORM	
61. NUMBER OF PAGES IN THIS COMPUTER CARD	
62. NUMBER OF PAGES IN THIS COMPUTER DISK	
63. NUMBER OF PAGES IN THIS COMPUTER TAPE	
64. NUMBER OF PAGES IN THIS OTHER	
65. NUMBER OF PAGES IN THIS SECTION	
66. NUMBER OF PAGES IN THIS APPENDIX	
67. NUMBER OF PAGES IN THIS TABLE	
68. NUMBER OF PAGES IN THIS DRAWING	
69. NUMBER OF PAGES IN THIS PLATE	
70. NUMBER OF PAGES IN THIS MICROFORM	
71. NUMBER OF PAGES IN THIS COMPUTER CARD	
72. NUMBER OF PAGES IN THIS COMPUTER DISK	
73. NUMBER OF PAGES IN THIS COMPUTER TAPE	
74. NUMBER OF PAGES IN THIS OTHER	
75. NUMBER OF PAGES IN THIS SECTION	
76. NUMBER OF PAGES IN THIS APPENDIX	
77. NUMBER OF PAGES IN THIS TABLE	
78. NUMBER OF PAGES IN THIS DRAWING	
79. NUMBER OF PAGES IN THIS PLATE	
80. NUMBER OF PAGES IN THIS MICROFORM	
81. NUMBER OF PAGES IN THIS COMPUTER CARD	
82. NUMBER OF PAGES IN THIS COMPUTER DISK	
83. NUMBER OF PAGES IN THIS COMPUTER TAPE	
84. NUMBER OF PAGES IN THIS OTHER	
85. NUMBER OF PAGES IN THIS SECTION	
86. NUMBER OF PAGES IN THIS APPENDIX	
87. NUMBER OF PAGES IN THIS TABLE	
88. NUMBER OF PAGES IN THIS DRAWING	
89. NUMBER OF PAGES IN THIS PLATE	
90. NUMBER OF PAGES IN THIS MICROFORM	
91. NUMBER OF PAGES IN THIS COMPUTER CARD	
92. NUMBER OF PAGES IN THIS COMPUTER DISK	
93. NUMBER OF PAGES IN THIS COMPUTER TAPE	
94. NUMBER OF PAGES IN THIS OTHER	
95. NUMBER OF PAGES IN THIS SECTION	
96. NUMBER OF PAGES IN THIS APPENDIX	
97. NUMBER OF PAGES IN THIS TABLE	
98. NUMBER OF PAGES IN THIS DRAWING	
99. NUMBER OF PAGES IN THIS PLATE	
100. NUMBER OF PAGES IN THIS MICROFORM	
101. NUMBER OF PAGES IN THIS COMPUTER CARD	
102. NUMBER OF PAGES IN THIS COMPUTER DISK	
103. NUMBER OF PAGES IN THIS COMPUTER TAPE	
104. NUMBER OF PAGES IN THIS OTHER	
105. NUMBER OF PAGES IN THIS SECTION	
106. NUMBER OF PAGES IN THIS APPENDIX	
107. NUMBER OF PAGES IN THIS TABLE	
108. NUMBER OF PAGES IN THIS DRAWING	
109. NUMBER OF PAGES IN THIS PLATE	
110. NUMBER OF PAGES IN THIS MICROFORM	
111. NUMBER OF PAGES IN THIS COMPUTER CARD	
112. NUMBER OF PAGES IN THIS COMPUTER DISK	
113. NUMBER OF PAGES IN THIS COMPUTER TAPE	
114. NUMBER OF PAGES IN THIS OTHER	
115. NUMBER OF PAGES IN THIS SECTION	
116. NUMBER OF PAGES IN THIS APPENDIX	
117. NUMBER OF PAGES IN THIS TABLE	
118. NUMBER OF PAGES IN THIS DRAWING	
119. NUMBER OF PAGES IN THIS PLATE	
120. NUMBER OF PAGES IN THIS MICROFORM	
121. NUMBER OF PAGES IN THIS COMPUTER CARD	
122. NUMBER OF PAGES IN THIS COMPUTER DISK	
123. NUMBER OF PAGES IN THIS COMPUTER TAPE	
124. NUMBER OF PAGES IN THIS OTHER	
125. NUMBER OF PAGES IN THIS SECTION	
126. NUMBER OF PAGES IN THIS APPENDIX	
127. NUMBER OF PAGES IN THIS TABLE	
128. NUMBER OF PAGES IN THIS DRAWING	
129. NUMBER OF PAGES IN THIS PLATE	
130. NUMBER OF PAGES IN THIS MICROFORM	
131. NUMBER OF PAGES IN THIS COMPUTER CARD	
132. NUMBER OF PAGES IN THIS COMPUTER DISK	
133. NUMBER OF PAGES IN THIS COMPUTER TAPE	
134. NUMBER OF PAGES IN THIS OTHER	
135. NUMBER OF PAGES IN THIS SECTION	
136. NUMBER OF PAGES IN THIS APPENDIX	
137. NUMBER OF PAGES IN THIS TABLE	
138. NUMBER OF PAGES IN THIS DRAWING	
139. NUMBER OF PAGES IN THIS PLATE	
140. NUMBER OF PAGES IN THIS MICROFORM	
141. NUMBER OF PAGES IN THIS COMPUTER CARD	
142. NUMBER OF PAGES IN THIS COMPUTER DISK	
143. NUMBER OF PAGES IN THIS COMPUTER TAPE	
144. NUMBER OF PAGES IN THIS OTHER	
145. NUMBER OF PAGES IN THIS SECTION	
146. NUMBER OF PAGES IN THIS APPENDIX	
147. NUMBER OF PAGES IN THIS TABLE	
148. NUMBER OF PAGES IN THIS DRAWING	
149. NUMBER OF PAGES IN THIS PLATE	
150. NUMBER OF PAGES IN THIS MICROFORM	
151. NUMBER OF PAGES IN THIS COMPUTER CARD	
152. NUMBER OF PAGES IN THIS COMPUTER DISK	
153. NUMBER OF PAGES IN THIS COMPUTER TAPE	
154. NUMBER OF PAGES IN THIS OTHER	
155. NUMBER OF PAGES IN THIS SECTION	
156. NUMBER OF PAGES IN THIS APPENDIX	
157. NUMBER OF PAGES IN THIS TABLE	
158. NUMBER OF PAGES IN THIS DRAWING	
159. NUMBER OF PAGES IN THIS PLATE	
160. NUMBER OF PAGES IN THIS MICROFORM	
161. NUMBER OF PAGES IN THIS COMPUTER CARD	
162. NUMBER OF PAGES IN THIS COMPUTER DISK	
163. NUMBER OF PAGES IN THIS COMPUTER TAPE	
164. NUMBER OF PAGES IN THIS OTHER	
165. NUMBER OF PAGES IN THIS SECTION	
166. NUMBER OF PAGES IN THIS APPENDIX	
167. NUMBER OF PAGES IN THIS TABLE	
168. NUMBER OF PAGES IN THIS DRAWING	
169. NUMBER OF PAGES IN THIS PLATE	
170. NUMBER OF PAGES IN THIS MICROFORM	
171. NUMBER OF PAGES IN THIS COMPUTER CARD	
172. NUMBER OF PAGES IN THIS COMPUTER DISK	
173. NUMBER OF PAGES IN THIS COMPUTER TAPE	
174. NUMBER OF PAGES IN THIS OTHER	
175. NUMBER OF PAGES IN THIS SECTION	
176. NUMBER OF PAGES IN THIS APPENDIX	
177. NUMBER OF PAGES IN THIS TABLE	
178. NUMBER OF PAGES IN THIS DRAWING	
179. NUMBER OF PAGES IN THIS PLATE	
180. NUMBER OF PAGES IN THIS MICROFORM	
181. NUMBER OF PAGES IN THIS COMPUTER CARD	
182. NUMBER OF PAGES IN THIS COMPUTER DISK	
183. NUMBER OF PAGES IN THIS COMPUTER TAPE	
184. NUMBER OF PAGES IN THIS OTHER	
185. NUMBER OF PAGES IN THIS SECTION	
186. NUMBER OF PAGES IN THIS APPENDIX	
187. NUMBER OF PAGES IN THIS TABLE	
188. NUMBER OF PAGES IN THIS DRAWING	
189. NUMBER OF PAGES IN THIS PLATE	
190. NUMBER OF PAGES IN THIS MICROFORM	
191. NUMBER OF PAGES IN THIS COMPUTER CARD	
192. NUMBER OF PAGES IN THIS COMPUTER DISK	
193. NUMBER OF PAGES IN THIS COMPUTER TAPE	
194. NUMBER OF PAGES IN THIS OTHER	
195. NUMBER OF PAGES IN THIS SECTION	
196. NUMBER OF PAGES IN THIS APPENDIX	
197. NUMBER OF PAGES IN THIS TABLE	
198. NUMBER OF PAGES IN THIS DRAWING	
199. NUMBER OF PAGES IN THIS PLATE	
200. NUMBER OF PAGES IN THIS MICROFORM	
201. NUMBER OF PAGES IN THIS COMPUTER CARD	
202. NUMBER OF PAGES IN THIS COMPUTER DISK	
203. NUMBER OF PAGES IN THIS COMPUTER TAPE	
204. NUMBER OF PAGES IN THIS OTHER	
205. NUMBER OF PAGES IN THIS SECTION	
206. NUMBER OF PAGES IN THIS APPENDIX	
207. NUMBER OF PAGES IN THIS TABLE	
208. NUMBER OF PAGES IN THIS DRAWING	
209. NUMBER OF PAGES IN THIS PLATE	
210. NUMBER OF PAGES IN THIS MICROFORM	
211. NUMBER OF PAGES IN THIS COMPUTER CARD	
212. NUMBER OF PAGES IN THIS COMPUTER DISK	
213. NUMBER OF PAGES IN THIS COMPUTER TAPE	
214. NUMBER OF PAGES IN THIS OTHER	
215. NUMBER OF PAGES IN THIS SECTION	
216. NUMBER OF PAGES IN THIS APPENDIX	
217. NUMBER OF PAGES IN THIS TABLE	
218. NUMBER OF PAGES IN THIS DRAWING	
219. NUMBER OF PAGES IN THIS PLATE	
220. NUMBER OF PAGES IN THIS MICROFORM	
221. NUMBER OF PAGES IN THIS COMPUTER CARD	
222. NUMBER OF PAGES IN THIS COMPUTER DISK	
223. NUMBER OF PAGES IN THIS COMPUTER TAPE	
224. NUMBER OF PAGES IN THIS OTHER	
225. NUMBER OF PAGES IN THIS SECTION	
226. NUMBER OF PAGES IN THIS APPENDIX	
227. NUMBER OF PAGES IN THIS TABLE	
228. NUMBER OF PAGES IN THIS DRAWING	
229. NUMBER OF PAGES IN THIS PLATE	
230. NUMBER OF PAGES IN THIS MICROFORM	
231. NUMBER OF PAGES IN THIS COMPUTER CARD	
232. NUMBER OF PAGES IN THIS COMPUTER DISK	
233. NUMBER OF PAGES IN THIS COMPUTER TAPE	
234. NUMBER OF PAGES IN THIS OTHER	
235. NUMBER OF PAGES IN THIS SECTION	
236. NUMBER OF PAGES IN THIS APPENDIX	
237. NUMBER OF PAGES IN THIS TABLE	
238. NUMBER OF PAGES IN THIS DRAWING	
239. NUMBER OF PAGES IN THIS PLATE	
240. NUMBER OF PAGES IN THIS MICROFORM	
241. NUMBER OF PAGES IN THIS COMPUTER CARD	
242. NUMBER OF PAGES IN THIS COMPUTER DISK	
243. NUMBER OF PAGES IN THIS COMPUTER TAPE	
244. NUMBER OF PAGES IN THIS OTHER	
245. NUMBER OF PAGES IN THIS SECTION	
246. NUMBER OF PAGES IN THIS APPENDIX	
247. NUMBER OF PAGES IN THIS TABLE	
248. NUMBER OF PAGES IN THIS DRAWING	
249. NUMBER OF PAGES IN THIS PLATE	
250. NUMBER OF PAGES IN THIS MICROFORM	
251. NUMBER OF PAGES IN THIS COMPUTER CARD	
252. NUMBER OF PAGES IN THIS COMPUTER DISK	
253. NUMBER OF PAGES IN THIS COMPUTER TAPE	
254. NUMBER OF PAGES IN THIS OTHER	
255. NUMBER OF PAGES IN THIS SECTION	
256. NUMBER OF PAGES IN THIS APPENDIX	
257. NUMBER OF PAGES IN THIS TABLE	
258. NUMBER OF PAGES IN THIS DRAWING	
259. NUMBER OF PAGES IN THIS PLATE	
260. NUMBER OF PAGES IN THIS MICROFORM	
261. NUMBER OF PAGES IN THIS COMPUTER CARD	
262. NUMBER OF PAGES IN THIS COMPUTER DISK	
263. NUMBER OF PAGES IN THIS COMPUTER TAPE	
264. NUMBER OF PAGES IN THIS OTHER	
265. NUMBER OF PAGES IN THIS SECTION	
266. NUMBER OF PAGES IN THIS APPENDIX	
267. NUMBER OF PAGES IN THIS TABLE	
268. NUMBER OF PAGES IN THIS DRAWING	
269. NUMBER OF PAGES IN THIS PLATE	
270. NUMBER OF PAGES IN THIS MICROFORM	
271. NUMBER OF PAGES IN THIS COMPUTER CARD	
272. NUMBER OF PAGES IN THIS COMPUTER DISK	
273. NUMBER OF PAGES IN THIS COMPUTER TAPE	
274. NUMBER OF PAGES IN THIS OTHER	
275. NUMBER OF PAGES IN THIS SECTION	
276. NUMBER OF PAGES IN THIS APPENDIX	
277. NUMBER OF PAGES IN THIS TABLE	
278. NUMBER OF PAGES IN THIS DRAWING	
279. NUMBER OF PAGES IN THIS PLATE	
280. NUMBER OF PAGES IN THIS MICROFORM	
281. NUMBER OF PAGES IN THIS COMPUTER CARD	
282. NUMBER OF PAGES IN THIS COMPUTER DISK	
283. NUMBER OF PAGES IN THIS COMPUTER TAPE	
284. NUMBER OF PAGES IN THIS OTHER	
285. NUMBER OF PAGES IN THIS SECTION	
286. NUMBER OF PAGES IN THIS APPENDIX	
287. NUMBER OF PAGES IN THIS TABLE	
288. NUMBER OF PAGES IN THIS DRAWING	
289. NUMBER OF PAGES IN THIS PLATE	
290. NUMBER OF PAGES IN THIS MICROFORM	
291.	